THE SNOWSCAT GROUND-BASED POLARIMETRIC SCATTEROMETER: CALIBRATION AND INITIAL MEASUREMENTS FROM DAVOS SWITZERLAND

Charles Werner[1], Andreas Wiesmann[1], Tazio Strozzi[1], Martin Schneebeli[2], Christian Mätzler(3)

(1) Gamma Remote Sensing, Gümligen, Switzerland;

http://www.gamma-rs.ch, cw@gamma-rs.ch

(2) WSL Institute for Snow and Avalanche Research Davos, Switzerland

(3) University of Bern, Institute of Applied Physics, Switzerland

The COld REgions Hydrology High-resolution Observatory (CoReH20) Mission proposes a dual frequency radar operating at 9.6 and 17 GHz utilizing VV and VH polarization [1]. By combining X- and Ku-Band with both co- and cross-polarization diversity it is possible to estimate the Snow Water Equivalent of dry snow. To support this proposed mission, ESA has sponsored the development of a ground-based coherent polarimetric scatterometer operating over the 9-18 GHz frequency range. ESA is supporting campaigns to acquire and process data using SnowScat for validation of Snow Water Equivalent (SWE) retrieval algorithms.

The SnowScat scatterometer is a fully polarimetric, coherent stepped-frequency CW radar that operates in the range of 9-18 GHz. Both angular and frequency diversity are used to obtain sufficient independent “looks” to reduce speckle noise and thus the uncertainty in the estimate of the radar backscatter $_0$. The instrument is mounted on the computer-controlled alt/azimuth 2-axis pan/tilt mount. The instrument is temperature regulated and fully weather sealed for installation in the alpine environment. SnowScat was deployed in late Winter 2009 on an 11m tower in a dedicated campaign at the Weissfluhjoch, Switzerland (Figure 1)[2][3].

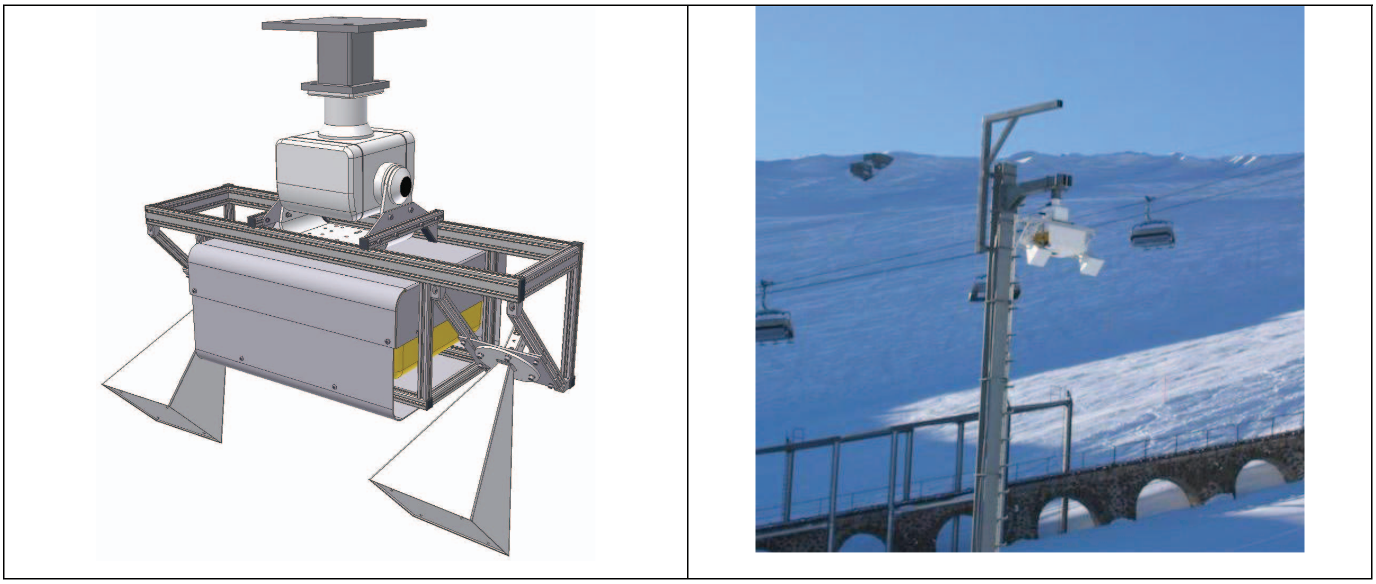

Figure 1: Snowscat showing antennas, electronics enclosure, and pan-tilt scanner.

SnowScat Data were collected continuously using quad-polarization over a thick snowpack (>2m) and in-situ measurements were performed for comparison and validation.

INSTRUMENT DESIGN

The scatterometer is a stepped frequency CW (SF-CW) radar covering 9-18 GHz. Figure 2 shows the system block diagram. The use of SF-CW permits precise frequency control and has distinct advantages for repeatability, simplicity of the design, cost, and calibration. The transmitted radar frequency during a measurement cycle is stepped in fixed increments (nominally 3072 kHz) over the frequency band. The synthesizer output is doubled in frequency to generate the scatterometer frequencies in the range of 9-18 GHz. The instrument uses dual-polarization 20 cm aperture horn antennas that have been characterized at the ESTEC Compact Antenna Test Range (CATR) over the 9-18 GHz frequency range. The use of these antennas supports fully polarimetric (HH, HV, VH, VV) measurements. The polarization purity of the antennas is rated at better than 22 dB.

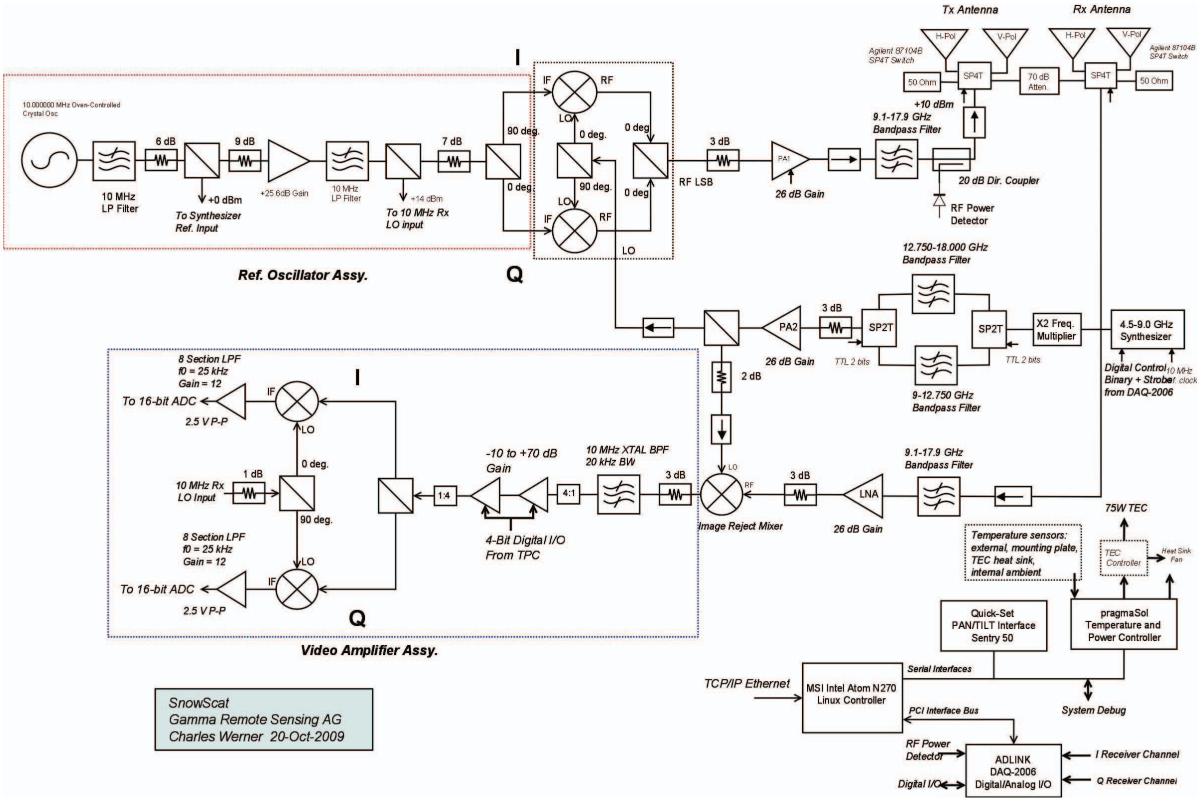

RADIOMETRIC CALIBRATION

Calibration of the scatterometer has two important goals. The primary goal is to obtain quantitatively accurate estimates of the backscatter coefficient σ_0. Second is to remove short term variations in the instrument gain, correcting frequency dependent errors in both amplitude and phase. SnowScat has an internal calibration loop where the transmitter output is fed through a calibrated path into the receiver. This path consists of short coaxial cable and 70 dB of attenuation. The calibration loop data can be used to correct temperature and time dependent variations in the instrument gain by measuring the instrument response apart from the antennas and feed cables. To further reduce temporal gain variations, the SnowScat has a temperature controller driving a thermoelectric element capable of both heating or cooling the scatterometer enclosure. During most of the campaign the internal temperature was kept at a constant 20C +/- 0.5C.

The frequency dependent power *S(f)*, measured by the scatterometer is given by the area radar equation:

$$S_r(f)=\frac{\lambda^2}{(4\pi)^3 k(f) L_a(f)}\iint\limits_{ill.area}\frac{G_T(f,\theta,\varphi)G_R(f,\theta,\varphi)\sigma_0(f,\theta,\varphi)}{r^4}dA \qquad (1)$$

where *k(f)* is the system calibration scale factor, $G_T()$ and $G_R()$ are the amplitude gain functions of the transmit and receive antennas, λ is the wavelength, *r* is the slant range, $L_a(f)$ is the calibration path loss, *A* is the area illuminated by the antennas on the ground, θ is the look angle, and ϕ is the antenna azimuth angle relative to boresight. An end-to-end calibration correction is measured using a spherical calibration target with known RCS:

$$\sigma'(f)=\frac{(4\pi)^3 r^4 L_a(f) S'_{cal}(f)}{G_T(f,0,0)G_r(f,0,0)\lambda^2} \qquad (2)$$

This is compared to the theoretical sphere RCS to measure an absolute power calibration factor:

$$k(f)=\frac{\sigma_{cal}(f)}{\sigma'(f)} \qquad (3)$$

Substituting for the differential area *dA* in terms of the observation geometry, the averaged normalized RCS over the footprint is given by :

$$\bar{\sigma}_0(f)=\frac{(4\pi)^3 S_r(f)k(f)L_a(f)h^2}{\lambda^2\iint\limits_{ill.area}G_T(f,\theta,\varphi)G_R(f,\theta,\varphi)\cos\theta\, d\theta\, d\phi} \qquad (4)$$

where *h* is the observation tower height. For each angle θ we can average over *N* independent observations to decrease the standard deviation of the measurements due to speckle, and terrain, and snow cover.

MEASUREMENT CAMPAIGN

Our test site is located at Weissfluhjoch and operated by the Swiss Federal Snow and Avalanche Research Institute. The measurement campaign began in late February and continued until April 2009. Absolute calibration was verified using a spherical calibration target located at approximately 8.3 meters from the scatterometer. An example of the calibration correction derived from the sphere calibration target is shown in Figure 3.

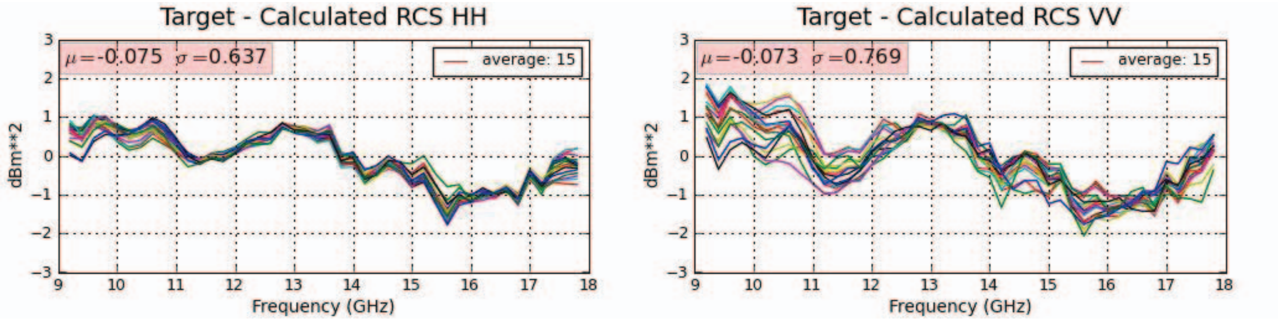

Figure 3. Calibration factor derived from 8” sphere backscatter measured over 9.5 to 17.5 GHz at a slant range of 8.3 m for 16 measurements acquired over a 24 hour period on 25-March-2009

An example of backscatter profiles for a 2m dry snow pack for incidence angles between 20 and 60 degrees are shown in Figure 4. As can be seen these single-look profiles have speckle noise. Independent range samples in these profiles have a spacing $\delta r = c/2B$ where *B* is the processing bandwidth. A processing bandwidth *B* of 1 GHz is used in order to obtain range looks $N_r \approx r\theta_{el}/\delta_r$ over the illuminated patch, where

r is the slant range and θ_{el} is the elevation antenna beamwidth. At each incidence angle the data are averaged in range and azimuth weighted by the product of the antenna patterns. The small bistatic squint angle between the antenna beams is taken into account for the integration over the illuminated antenna footprint.

CONCLUSIONS

We present the first results from calibration of the SnowScat scatterometer that operated at Weissfluhjoch during the Winter season of 2009. The instrument has been designed to operate in severe alpine environments. SnowScat has acquired a data set that will be used for validation of SWE retrieval algorithms in support of the CoReH20 mission. Processing and calibration of the entire Weissfluhjoch data set is ongoing.

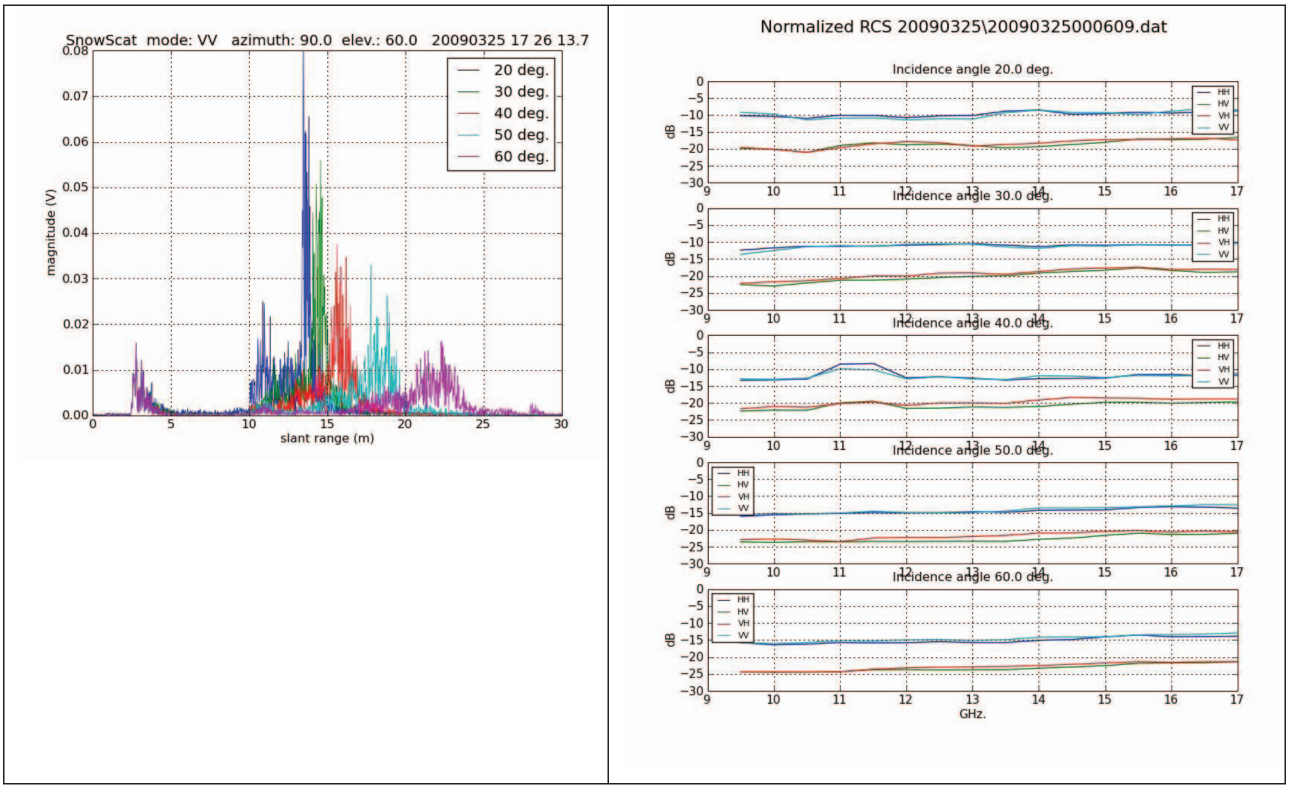

Figure 4 (a)VV Range profiles at incidence angles ranging from 20 to 60 degrees. Signal at the left is cross-coupling clutter between the antennas that is removed by range-gating. (b)Calibrated normalized
ranged between -13 and -5 C.

ACKNOWLEDGMENTS

The fabrication of the stepped frequency scatterometer and the field campaigns are supported by ESA through ESA-ESTEC AO/1-5311/06/NL/EL. Special thanks to Björn Rommen of ESTEC for his leadership, support, and scientific advice. We also want to thank Luis Rolo of the ESTEC Antenna and Sub-Millimetre Wave Section for precise measurements of the antennas and complete SnowScat instrument.

REFERENCES

[1] Rott, H., Cline, D., Duguay, C., Essery, R., Haas, C., Macelloni, G., Malnes, E., Pulliainen, J., Rebhan, H., Yueh, S.(2008). CoReH2O - A Ku- and X-Band SAR Mission for Snow and Ice Monitoring, EUSAR 2008 Proceedings, Paper 5.2.2, 7th European Conference on Synthetic Aperture Radar, June 2-5, 2008,Friedrichshafen, Germany.

[2] Mätzler C., "Applications of the Interaction of Microwaves with the Natural Snow Cover", Remote Sensing Reviews, Vol. 2, pp. 259-392 (1987).

[3] Strozzi T., A. Wiesmann and C. Mätzler, Active Microwave Signatures of Snowcovers at 5.3 and 35 GHz. Radio Science, Vol. 32, No. 2, pp. 479-495, 1997.